XLIII CILAMCE
21–25, November, 2022
FOZ DO IGUAÇU – PR – BRAZIL

Numerical analysis of the bifurcation point sensibility to the temperature field in the Taylor-Couette flow

Henrique Queiroz Rodrigues[1], André Yudi Kiatake Kamiya[1], Julien Pellé[2], Thiago Antonini Alves [3], Fernando Augusto Alves Mendes [1], Augusto Salomão Bornschlegell[1]

[1]*Faculty of Engineering, University of Grande Dourados*
Rodovia Dourados - Itahum, Km 12 - Cidade Universítária, 79804970, Mato Grosso do Sul, Brazil
henrique.rodrigues062@academico.ufgd.edu.br, andre.kamiya705@academico.ufgd.edu.br, fernandomendes@ufgd.edu.br, augustosalomao@ufgd.edu.br
[2]*Laboratory of Automation, Mechanics, Industrial and Human Computer Science, Université Polytechnique Hauts-de-France*
Campus Mont Houy, 59313 Valenciennes cedex 9, France
jpelle@uphf.fr
[3]*Dept. of Mechanical Engineering, Federal University of Technology-Paraná*
R. Doutor Washington Subtil Chueire, 330-Jardim Carvalho, 84017-220, Ponta Grossa-PR, Brazil
antonini@utfpr.edu.br

Abstract. The flow between concentric cylinders, called Taylor-Couette flow, has been extensively studied during last century in works describing its governing parameters and presenting the various flow regimes for each configuration. This kind of flow is present in the air gap of electrical machines and its characteristics affect the heat transfer and the torque generated on the outer cylinder due viscous forces. The intensity of these effects depends on the flow state, which is governed by geometric characteristics and Reynolds number. Our objective is to analyze the effect of heat transfer on the surging wavy vortex and on the torque generated at outer cylinder. The numerical simulations are done using the software OpenFOAM v9 with K-Omega SST as the main turbulence model. All the simulations were in the transient regime. The pisoFoam solver was employed for the isothermal problem and for the buoyantPimpleFoam solver for the thermal problem. A mesh independence study was done based on Grid Convergence Index (GCI) method, where we found satisfactory values. For the thermal cases, we analyzed the behavior of the flow as we increase the Reynolds number and the temperature at the walls, comparing its results with the isothermal. It is notable the delay in the formation of the wavy vortices comparing with the rotational speed and the decrease of the torque on the external wall.

Keywords: Taylor-Couette, CFD, Bifurcation

1 Introduction

A Taylor-Couette flow is a flow condition where the fluid is confined beetween two coaxial cylinders at different angular velocities. In this work, the outer cylinder is static and the inner rotates. The main characteristic of this type of flow is the presence of counter-rotating vortices that appear under certain conditions, which are called Taylor vortices.

Taylor-Couette flow (TC) is seen between the rotor and stator of an electrical machine, see Fig. 6(b). The flow characteristics alters the convective coefficient of the region, which affects the heat dissipation inside the electric machine. It can directly interfere in the efficiency and useful life of the device, as presented in Dauner [2] and Lancial [3]. The Taylor-Couette flow is also applied in concentric cylinder viscometer, which was first time studied by Maurice Couette [4]. He was the first to measure the viscosity of different fluids from a flow in the concentric cylinder geometry. He applied the flow conditions on Navier-Stokes equations, then he arrived at the relations to obtain the fluid viscosity from the flow in annular regions. Taylor [5] contains the first description of linear stability theory for general cases of viscous flow and his paper also contains a description of his experimental apparatus, which made possible for the first time photographs the different states of the flow.

In 1985, Andereck and Swinney [6] studied the large variety of different flow states and their respective

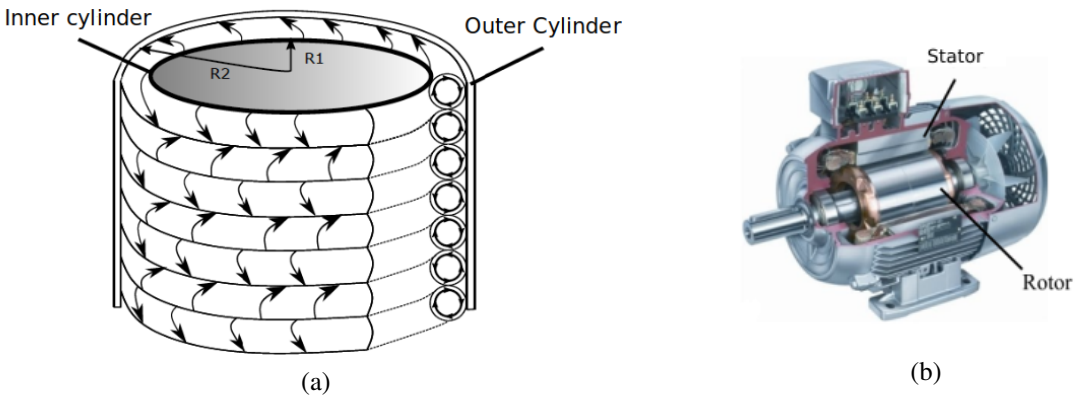

Figure 1. (a) Representation of Taylor-Couette vortices. (b) Rotor and stator at an electrical machine [1]

transition points, including the wavy vortex flow (WVF) that is the next state after linear Taylor vortices. At this state, the Taylor vortices become unstable and they loses their axysymmetric pattern.

Many studies has been done about the effects of radial heating on Taylor-Couette stability, like Liu [7], Masuda [8] and Hosain [9]. Their results shows that the instability of the vortices enhance the overall heat transfer. Another example is Fenot [10], where he presents the main parameters that govern the flow. More recently Leng [11], presented a study with axial temperature gradient for a large range of Reynolds number (R_e), defined in Eq. (1). Where Ω_1 is the angular velocity (rad/s) of the inner cylinder, R_1 and R_2 are the radii (m) of the inner and outer cylinder respectively, D is the gap (m) between the cylinders and υ is the kinematic viscosity (m^2/s) of the fluid.

$$Re = \frac{\Omega_1 R_1 D}{\upsilon}. \tag{1}$$

η is the gap width between the inner radii and outer radii (R_1/R_2) of the cylinders. It is an important parameter to compare the results with other works in the literature.

The fluid movement generates a torque G $(N.m)$ at the outer cylinder. At low angular velocity of the inner cylinder, before the formation of the vortices, the torque varies linearly with the rate of rotation, as presented by Donnely[12] in Eq.2, where G_{lam} is the torque $(N.m)$ at the laminar regime, ρ is the density (kg/m^3) of the fluid and L is the length (m) of the section.

$$G_{lam} = \frac{4\pi\rho\upsilon R_1^2 R_2^2 L\Omega_1}{R_2^2 - R_1^2}. \tag{2}$$

To evaluate G_{lam} it was used the air properties ρ and υ at the mean temperature between the walls.

Dubrulle [13] introduced a relevant dimensionless quantity, the non-dimensional angular momentum transfer (Nu_w), which is the ratio between the measured (G) and the laminar (G_{lam}) torque. According to Eckhardt[14], Nu_w measures how effective the transverse convective angular moment transport is in terms of the purely molecular transverse transport.

$$Nu_w = \frac{G}{G_{lam}}. \tag{3}$$

For WVF purely turbulent, Dubrulle [13] shows that there is no power law dependence of the torque versus Reynolds, there are only logarithmic corrections to the regime. The point where the real torque deviates from the linear behavior is called bifurcation point, which corresponds to the critical Reynolds number R_{cr}. This is interpreted as the onset of instability that generates the Taylor vortices. In addition to Dubrulle [13], many other works studied the relation between torque and rotational speed, among then we can mention Lewis [15] and Grossmann [16], who analyzed the torque as a function of the number of vortices and their oscillation frequency.

Our main objective is to numerically analyze the effects of different temperature configurations on the point of surging wavy vortices and their effect on the torque generated at the outer cylinder.

2 Numerical model

The numerical simulations were modeled using the software OpenFOAM at the version 9.0. This is a open source software that use C++ language program. It allow us to explore different solvers, turbulence models and many possibilities for post processing.

2.1 Geometry, mesh and boundary conditions

The present numerical model represents the flow in the region between the rotor and stator of an electrical machine, with one millimeter gap and 70 millimeter inner radius, what makes $\eta = 0.986$. At the axial direction (z), the modeled length is 20 mm.

In order to represent the flow second instability (WVF) with the available computational resources, instead of representing the whole perimeter (360 degrees), we have arbitrary modeled 1/24 th, that is, 15 degrees. At the faces where the flow should be continuous in the real case (orthoradial direction), it was applied the cyclic boundary condition (i.e. one surface is connected to another). The lateral faces as well as the stator are set as walls with no-slip boundary condition. The inner radius was set as wall with the rotational boundary condition. The geometry is presented at Fig.2.

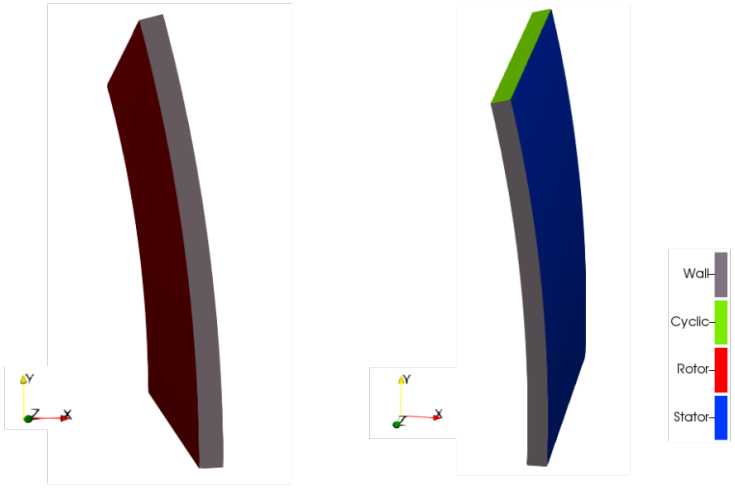

Figure 2. Geometry and patches

The mesh has 258,944 cells, 14 cells at r direction, 136 cells for θ and z direction. An expansion ratio was applied at the r direction intending to better represent the boundary layer in the simulation (i.e. the cells near the cylinder walls are narrower), see Fig. 3(b).

2.2 Mesh independence

Intending to analyze the capacity of our mesh to generate a consistent result, we did a mesh independence test, based on Grid Convergence Index (GCI) method, proposed by Celik [17]. This method compares the variation of an representative variable (ϕ) of the flow with the mesh refinement. As we increase the mesh refinement, the value of the variable shall converge. For all meshes, the flow's structure and the transient behavior were the same. Then, it was used two variables, the average torque (ϕ_1) at the stator and the oscillation frequency of the pressure (ϕ_2) obtained by FFT algorithm. Table 1, compares ϕ_1 and ϕ_2 for the meshes N1 (finner), N2 (average) and N3 (coarser). Comparing the meshes N2 and N1 we observe that GCI for both variables are below 0,5%, whereas comparing N2 and N3 the GCI is below 1.5%. Then, N2 mesh was selected in the present study.

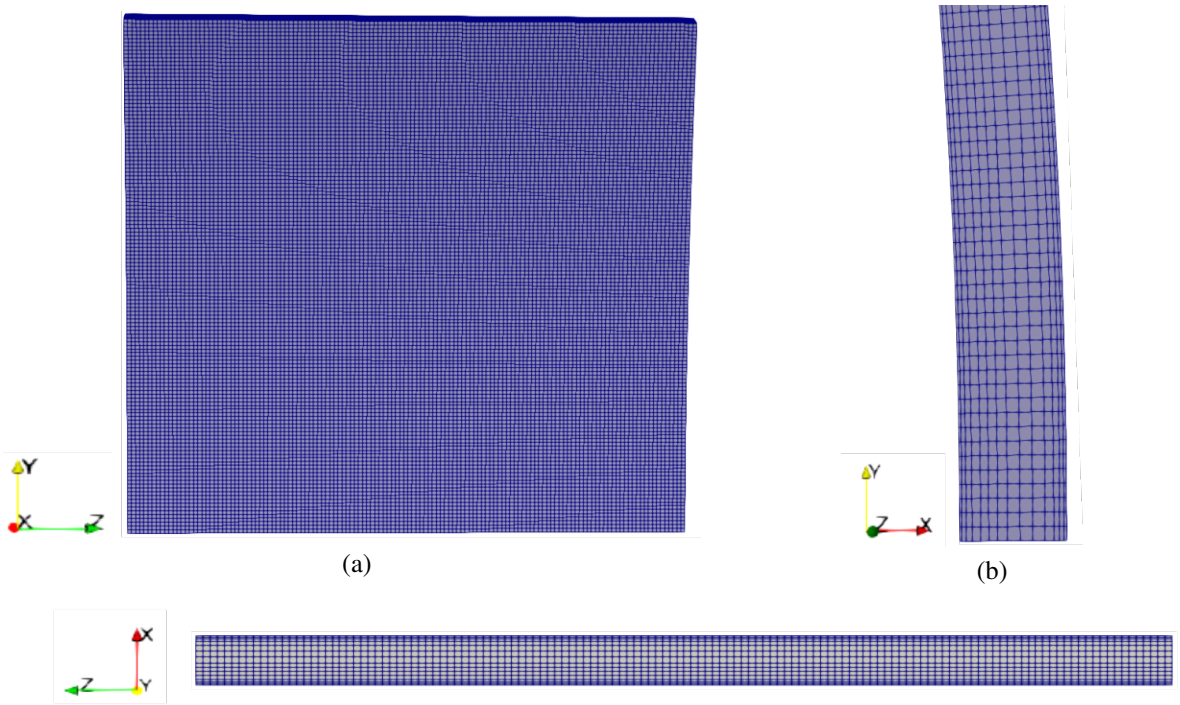

Figure 3. (a) Front view of the mesh. (b) Close-up view of side face. (c) Cyclic face.

Table 1. Results for GCI method

	ϕ=Average torque $(N \cdot m)$	ϕ=Oscillation frequency (Hz)
N_1, N_2, N_3	575,244, 258,944, 116,699	575,244, 258,944, 116,699
r_{21}, r_{32}	1.3, 1.3	1.3, 1.3
ϕ_1	$8.45E^{-05}$	277.4
ϕ_2	$8.66E^{-05}$	277.5
ϕ_3	$8.73E^{-05}$	284
e_a^{21}, e_a^{32}	0.8%, 2.5%	0.04%, 2.3%
GCI^{21}	0.5%	0.0007%
GCI^{32}	1.5%	0.045%

2.3 Solver, turbulence model and simulation parameters

The flow was modelled using the pisoFoam transient solver for the isothermal case and bouyantPimpleFoam for the thermal cases. SST K-Omega is the turbulence model applied on the simulation, always with a 5% turbulent intensity. The relaxation factors applied for pressure and velocity fields were set to 0.7 and 0.9, respectively. The temporal discretization (Δ_t) was defined by CFL condition, Courant [18], for any case the Courant number(C_r) must be equal or smaller than 1. The time scheme used is the backward scheme and the initial condition is zero velocity field.

We evaluated fours cases. The first case, case 1, the flow is isothermal. In Case 2, the rotor and stator boundary conditions are, respectively, imposed temperature of 400 K and 300 K, in this case the heat flux varied between 3000 and 4000 ($W.m^2$). In Case 3, the imposed temperature at the rotor and stator are, respectively, 500 K and 300 K, in this case the heat flux varied between 7000 and 8000 ($W.m^2$). In Case 4, a heat flux of 1000 W/m^2 is imposed at the rotor, at the the stator, a fixed temperature of 300 K. For cases 2,3 and 4, the lateral walls are considered adiabatic.

3 Results and discussion

The transition to WVF was visually identified by the pressure field for all cases. As we can see at Fig. 4 (a), its still laminar TC and, at Fig. 4 (b), its already a WVF.

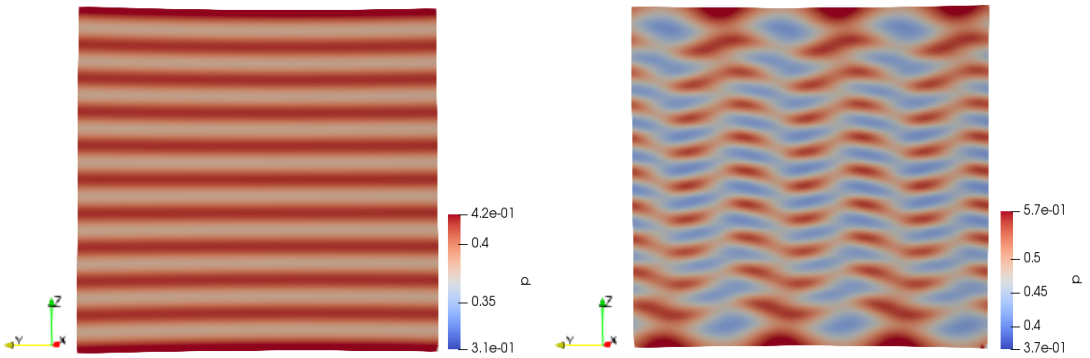

(a) (b)

Figure 4. Pressure field (Pa) on inner cylinder, isothermal case, (a) 60 rad/s (b) 66 rad/s

Figure 6 illustrates the torque at the outer cylinder for all the four studied cases and their two transitions point: the formation of TC vortices and the beginning of WVF. Analyzing cases 1, 2 and 3, we can see that, adding heat, the transition occurs later in relation to angular speed but earlier in relation to Re. It occurs because the air viscosity increases with the enhance of temperature, decreasing Re. These transition results correspond to Liu's [7] work.

In all the cases, the bifurcation point match with the appearance of the Taylor-Couette vortices. The torque keeps with its new linear behavior for a small range of Re and then have a smooth and slight slope change when the wavy vortex begins. This characteristic is highlighted by the red marks at Nu_w graphic in Fig 7 (a). Figure 7 (b) presents the result from Arias [19], to compare the Nu_w behavior. We can see that for the cases where η is closer to our work ($\eta = 0.986$), the behavior is pretty similar.

It is worth to mention that the difficulty of determining the viscosity and density of the air in the flow may cause an uncertainty in G_{lam} and G estimate before the formation of Taylor-Couette vortices.

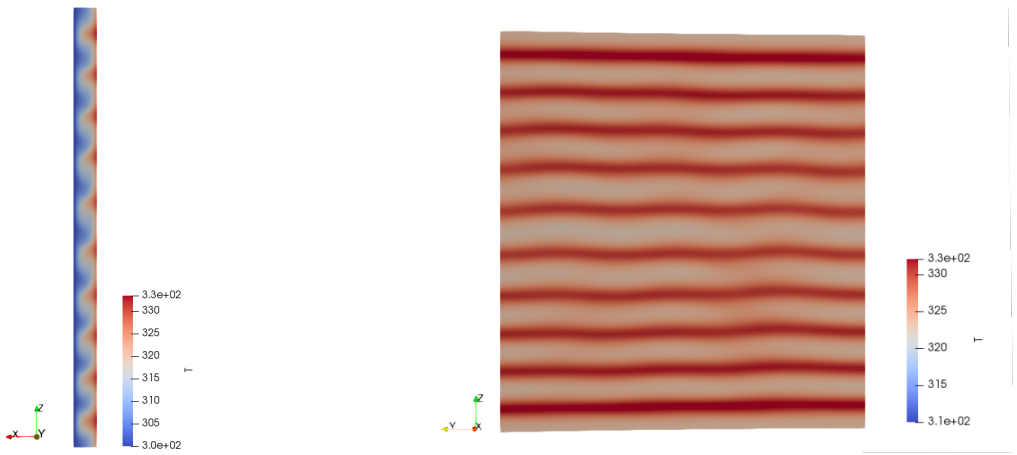

(a) (b)

Figure 5. Rotor surface temperature (K) distribution-Case 4, 120 rad/s, t=0.5 s, (a) X-Z plane (b) Y-Z plane

For the case with heat flux (case 4), we can see Taylor vortices effect on the surface temperature of the inner cylinder, see Fig. 5 (b). The periodic distribution with 10 °C of temperature variation is expected, as observed by

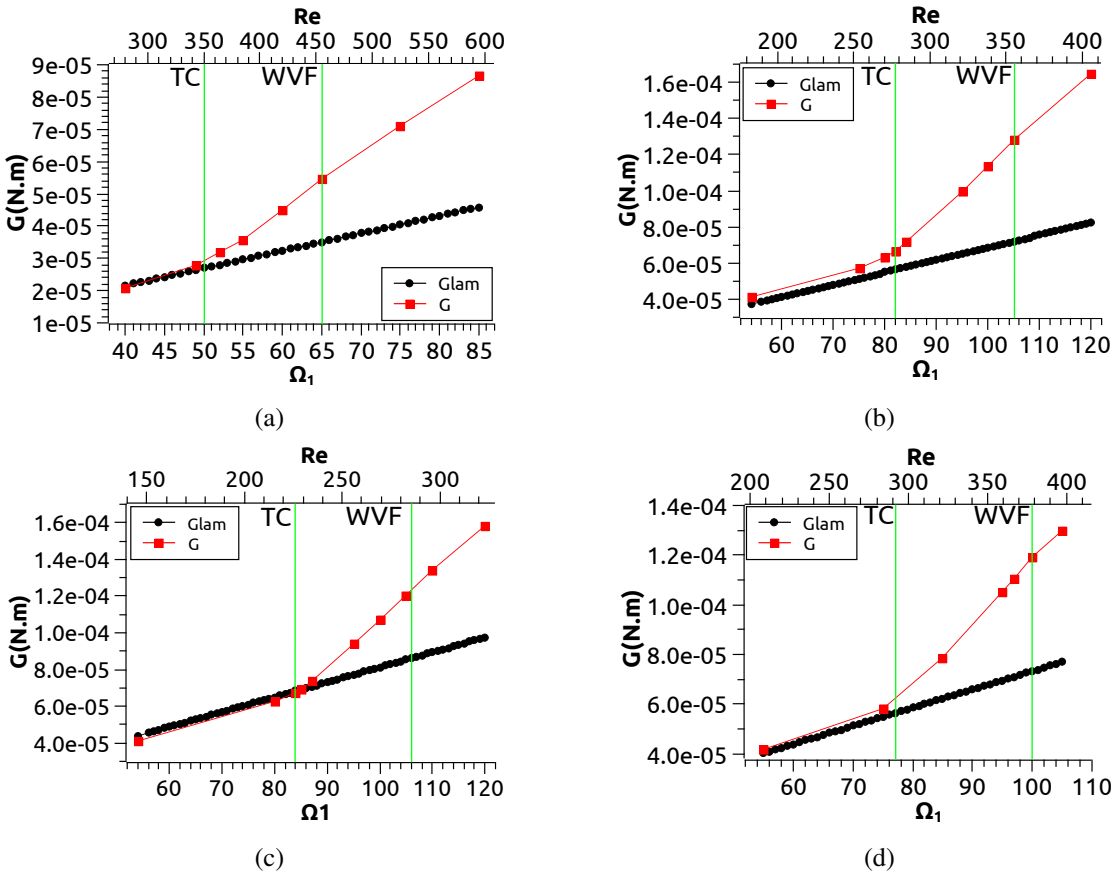

Figure 6. Torque scaling with Re, (a) Case 1, (b) Case 2, (c) Case 3, (d) Case 4

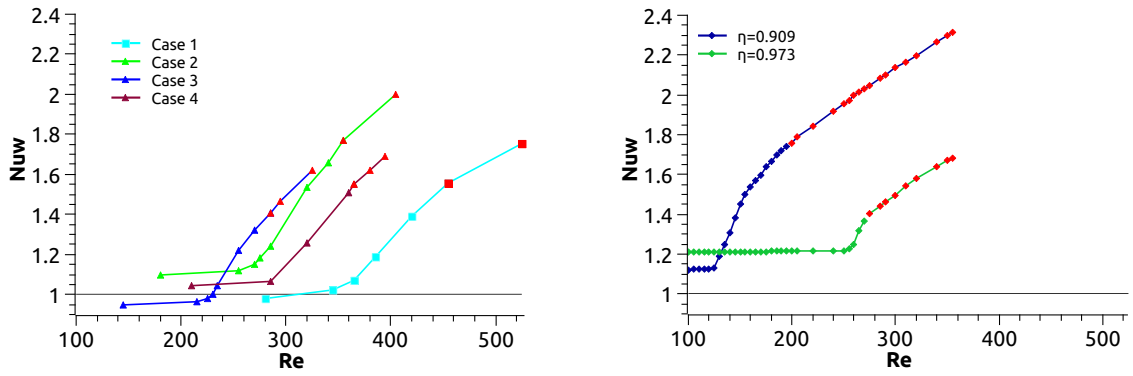

Figure 7. (a) Nu_w of the four studied cases, with fixed gap width, $\eta = 0.986$, (b) Nu_w for two different gap widths [Arias [19]]. The red marks represents the wavy vortex flow region

Hosain [20], but for the early wavy vortex is seen also an smooth oscillation on the lines of temperatures, which is caused by the linearity and low oscilation frequency of the vortice cells.

4 Conclusions

The transition to wavy vortex flow occurs for cases 1, 4 ,2 and 3 (increasing heat flux) respectively at 65, 100, 105 and 106 rad/s. Observing the Reynolds number, the same transition occurs at 455, 378, 355 and 285. So we can see that adding heat on a Taylor-Couette flow, with the given geometry, it delays the transitions only in relation

to the angular velocity, but observing Re, the effect is opposite (i.e. Re decreases). In contrast to the TC formation, which defines the bifurcation point, the formation of the WVF has a slight influence to the torque behavior.

Authorship statement. The authors hereby confirm that they are the sole liable persons responsible for the authorship of this work, and that all material that has been herein included as part of the present paper is either the property (and authorship) of the authors, or has the permission of the owners to be included here.

References

[1] Comparé thermique Le moteur - Mediachimie. [Online; accessed 11. Jul. 2022], 2022.
[2] F. A. Dauner. *Determinação Numérico-Experimental de Expressões Analíticas para a Avaliação do Coeficiente Convectivo no Interior de um Motor Elétrico Fechado*. PhD thesis, Universidade do Estado de Santa Catarina, 2019.
[3] F. B. S. H. F. Torriano. N. Lancial and G. Rolland. Taylor-couette-poiseuille flow and heat transfer in an annular channel with a slotted rotor. *International Jourlan of Thermal Sciences*, vol. 112, pp. 92–103, 2017.
[4] M. Couette. Sur un nouvel appareil pour l'étude du frottement des fluides. *CR Acad Sci*, vol. 107, pp. 388–390, 1888.
[5] G. I. Taylor. Stability of a viscous liquid contained between two rotating cylinders. *Philosophical transactions of the royal society of london*, vol. 223, pp. 289–343, 1923.
[6] C. D. Andereck and H. L. Swinney. Flow regimes in a circular couette system with independently rotating cylinders. *Journal of Fluid Mechanics*, vol. 164, pp. 155–183, 1986.
[7] J. C. I. Kang. D. Liu and H. Kim. Experimental study on radial temperature gradient effect of a taylor-couette flow with axial wall slits. *Experimental Thermal and Fluid Science*, vol. 35, pp. 1282–1292, 2011.
[8] T. O. S. Yoshida. H. Masuda and M. Shimoyamada. Flow dynamics in taylor-couette flow reactor with axial distribution of temperature. *American Institute of Chemical Engineers*, vol. 0, 2017.
[9] M. L. Hosain and R. B. Fdhila. Air-gap heat transfer in rotating electrical machines: A parametric study. *Energy Procedia*, vol. 142, pp. 4176–4181, 2017.
[10] E. D. Y. Bertin. M. Fénot and G. Lalizel. A review of heat transfer between concentric rotating cylinders with of without axial flow. *International Jourlan of Thermal Sciences*, vol. 50, pp. 1138–1155, 2011.
[11] x.Y. D. K. Leng and J. Q. Zhong. Flow structures and heat transport in taylor-couette systems with axial temperature gradient. *Journal of Fluid Mechanics*, vol. 920, 2021.
[12] R. J. Donnely and N. J. Simon. An empirical torque relation for supercritical flow between rotating cylinders. *Journal of Fluid Mechanics*, vol. 7, pp. 401–418, 1960.
[13] B. Dubrulle and F. Hersant. Momentum transport and torque scaling in taylor-couette flow from an analogy with turbulent convection. *The European Physical Journal B*, vol. 26, pp. 379–386, 2002.
[14] S. G. B. Eckhardt and D. Lohse. Torque scaling in turbulent taylor-couette flow between independently rotating cylinders. *Journal of Fluid Mechanics*, vol. 581, pp. 221–250, 2007.
[15] G. S. Lewis and H. L. Swinney. Velocity structure functions, scaling, and transitions in high-reynolds-number couette-taylor flow. *Physical Review E*, vol. 59, n. 5, pp. 5458–5467, 1999.
[16] S. Grossmann, D. Lohse, and C. Sun. High–reynolds number taylor-couette turbulence. *Annual Review of Fluid Mechanics*, vol. 48, n. 1, pp. 53–80, 2016.
[17] P. J. R. C. J. F. H. C. U. Ghia. I. B. Celik and P. E. Raad. Procedure for estimation and reporting of uncertainty due to discretization in cfd applications. *Journal of Fluid Mechanics*, vol. 130, n. 7, 2014.
[18] K. F. R. Courant and H. Lewy. Uber die partiellen differenzengleichungen der mathematischen physik. *Mathematische Annalen.*, vol. 100, pp. 32–74, 1928.
[19] B. M. Arias. Torque measurement in turbulent couette-taylor flows. *Université du Havre*, 2015.
[20] R. B. F. M.D. L. Hosain and K. Roonberg. Taylor-couette flow and transient heat transfer inside the annulus air-gap of rotating electrical machines. *Applied Energy*, vol. 207, pp. 624–633, 2017.